Published in final edited form as:
J Immunol. 2014 March 15; 192(6): 2920–2931. doi:10.4049/jimmunol.1302801.

Oxidized lipids block antigen cross-presentation by dendritic cells in cancer1 Oxidized lipids and DCs in cancer

Wei Cao[†,*], **Rupal Ramakrishnan**[†,*], **Vladimir A. Tuyrin**[‡], **Filippo Veglia**[§], **Thomas Condamine**[§], **Andrew Amoscato**[†], **Dariush Mohammadyani**[¶], **Joseph J. Johnson**[‖], **Lan Min Zhang**[#], **Judith Klein-Seetharaman**[**], **Esteban Celis**[†], **Valerian E. Kagan**[‡], and **Dmitry I. Gabrilovich**[†,§,††]

[†]Department of Immunology, H. Lee Moffitt Cancer Center and Research Institute, Tampa, FL, 33612

[‖]Department of Microscopy Core, H. Lee Moffitt Cancer Center and Research Institute, Tampa, FL, 33612

[#]Department of Molecular Core of H. Lee Moffitt Cancer Center and Research Institute, Tampa, FL, 33612

[‡]Department of Environmental and Occupational Health, University of Pittsburgh, PA, 15219

[¶]Department of Bioengineering, University of Pittsburgh, PA, 15219

[§]The Wistar Institute, Philadelphia, PA, 19104

[**]Division of Metabolic and Vascular Health, Medical School, University of Warwick, Coventry CV4 7AL, UK

Abstract

Cross-presentation is one of the main features of dendritic cells DCs, critically important for the development of spontaneous and therapy-inducible antitumor immune responses. Patients, at early stages of cancer, have normal presence of DCs. However, the difficulties in the development of antitumor responses in patients with low tumor burden raised the question of the mechanisms of DC dysfunction. In this study, we found that, in differentiated DCs, tumor-derived factors blocked the cross-presentation of exogenous antigens without inhibiting the antigen presentation of endogenous protein or peptides. This effect was caused by intracellular accumulation of different types of oxidized neutral lipids: triglycerides, cholesterol esters, and fatty acids. In contrast, the accumulation of non-oxidized lipids did not affect cross-presentation. Oxidized lipids blocked cross-presentation by reducing the expression of peptide-MHC class I complexes on the cell surface. Thus, this study suggests the novel role of oxidized lipids in the regulation of cross-presentation.

[1]This work was supported by NIH grant CA165065 to DIG and VEK and R01CA136828 to EC

[††]address for correspondence: Dmitry Gabrilovich, The Wistar Institute, Rm. 118, 3601 Spruce Str. Philadelphia, PA, 19104, Ph. 215-495-6955, dgabrilovich@wistar.org.
[*]contributed equally to this work

Introduction

Antitumor immune responses, either spontaneous or induced by immune therapy, depend on the adequate function of host dendritic cells (DCs) (1-3). Defects in DC function in tumor-bearing (TB) patients or mice, with advanced disease, are well documented. They manifest in the expansion of immature DCs, unable to properly present antigen, and the generation of cells with immune suppressive activity, including regulatory DCs and myeloid-derived suppressor cells (MDSCs) (4). Together with other immune suppressive factors those changes contribute to the inability of cytotoxic T lymphocytes (CTLs) to mount antitumor immune responses (5-8).

Cross-presentation of antigens is a unique feature of DCs, which is critically important for antitumor immunity. Cross-presentation is the process where exogenous antigens are ingested and processed to generate peptide T cell epitopes that are presented by MHC class I (MHC-I) molecules (9, 10). Currently, two main pathways of cross-presentation have been described: cytosolic and vacuolar. Following uptake, exogenous antigens are internalized into phagosomes or endosomes (11, 12). The cytosolic pathway involves the transfer of exogenous antigen from the endosome/phagosome into the cytosol for proteasomal degradation. Similar to direct presentation, this pathway is dependent on the transporter for antigen presentation (TAP). In contrast, the vacuolar pathway is TAP independent and suggests that exogenous proteins are degraded into peptides by lysosomal proteases within the phagosome (or endosome). These peptides are then loaded onto MHC-class I molecules that recycle through the endocytic compartments by peptide exchange. The use of each pathway may depend on the type of antigen, and the mechanism of its uptake.

The main paradigm of tumor immunology stipulates that the efficient CTL priming requires an uptake of tumor antigens by DCs, their migration to draining lymph nodes, and a cross-presentation of the antigens to $CD8^+$ T cells in the context of MHC-class I (13). DCs from TB mice are able to cross-present tumor antigen to CTLs (14-17). DC infiltration of solid tumors is well documented in TB patients and mice (18-21). Tumor growth is associated with tumor cell apoptosis and necrosis and DCs have access to a large amount of tumor antigens via numerous mechanisms such as, phagocytosis/endocytosis of cell associated or soluble antigens bound to heat shock proteins (HSP), as well as via gap junction transfer, through the capture of exosomes, or via “cross-dressing” (acquisition of peptide MHC-I complexes from contact with necrotic cells) (22, 23). The tumor milieu contains soluble mediators such as type-I IFN, and endogenous “danger signals” (DNA, HMGB1, S100), which are able to activate DCs. Taken together, all of these factors induce DC differentiation and activation. However, this does not result in the development of potent antitumor immune responses. Moreover, the induction of strong immune responses to cancer vaccines is a difficult task, even in patients with a relatively small tumor burden.

In this study, we tried to address this question by studying the effect of tumor-derived factors (TDF) on partially differentiated DCs. We found that TDF inhibited the cross-presentation of exogenous proteins and long peptides, requiring antigen processing in DCs; without affecting the presentation of endogenous proteins and directly loaded short/minimal MHC-I binding peptides. Recently, lipid droplets or lipid bodies (LBs) were implicated in

cross-presentation via their association with ER-resident 47 kDa immune-related GTPase, Igtp (Irgm3) (24). LBs are neutral lipid storage organelles present in all eukaryotic cells. It is now established that LBs perform functions beyond lipid homeostasis. In addition, LBs were implicated in the regulation of immune responses via prostaglandins and leukotrienes and, possibly, in interferon responses (rev. in(25)). Under physiological conditions in most cells, LBs are rather small with a diameter ranging from 0.1 to 0.2μm (26). In the tumor microenvironment, DCs accumulate lipids and form large LBs (27), which we hypothesized could directly interfere with cross-presentation. We present the results indicating that cross-presentation is directly regulated by the oxidized lipids that accumulate in DCs.

Material and Methods

Human cells, mice and tumor models

Donors' buffy coat blood was purchased from the local blood bank. Animal experiments were approved by University of South Florida Institutional Animal Care and Use Committee. Balb/c or C57BL/6 mice were obtained from the National Cancer Institute. OVA transgenic mice C57BL/6-Tg(CAG-OVA)916Jen/J (Cat: 005145), CD204 knockout mice B6.Cg-Msr1^{tm1Csk}/J (Cat: 006096), mice on high fat diet (60 kcal% DIO high fat diet, Cat: 380050) and the same age control mice (10 kcal% DIO controls, Cat: 380056) were purchased from Jackson Laboratory. OT-I TCR-transgenic mice (C57Bl/6-Tg(TCRaTCRb)1100mjb) were obtained from Jackson Lab. Pmel-1 TCR-transgenic mice (B6.Cg Thy1^{a}-Tg(TcraTcrb)8Rest/J) were kindly provided by Dr. N. Restifo.

Reagents and cell lines

Tumor cell lines including CT26 and MC38 colon carcinomas, EL4 lymphoma, LLC (Lewis Lung Carcinoma), and B16F10 melanoma were maintained in RPMI-1640 medium supplemented with 10% fetal bovine serum (FBS, Sigma-Aldrich, St. Louis, MO) at 37°C, 5% CO_2. Tumors were injected subcutaneously (s.c.) at 5×10^5 cells per mouse.

SIINFEKL peptide, control peptide RAHYNIVTF, (Pam)2-KMFV-E-SIINFEKL peptide (derived from OVA) and (Pam)2-KMFV-KVPRNQDWL (derived from gp100) were obtained from American Peptide Company (Vista, CA). Ovalbumin (lyophilized powder, ≥98% agarose gel electrophoresis, Cat: A5503) was purchased from Sigma. Recombinant mouse GM-CSF was obtained from Biosource, Invitrogen Corp., Carlsbad, CA. recombinant human GM-CSF and IL-4 were obtained from CellGenix. Biotin conjugated anti mouse CD11c antibody (Cat: 553800) was purchased from BD Biosciences and used for DCs purification. In addition, FITC (Cat: 553801) or APC (Cat: 550261) or PE-Cy7 (Cat: 558079) conjugated anti mouse CD11c antibodies were obtained from BD Biosciences. Both FITC conjugated anti mouse MHC-I (H2Kb) antibody (Cat: 11-5958-82) and APC conjugated anti mouse SIINFEKL-H2Kb complex antibody (Clone: 25-D1.16, Cat: 17-5743-82) were purchased from eBioscience. In addition, variant fluorescent conjugated antibodies including APC conjugated anti mouse MHC-II (IAb) antibody (Cat: 17-5321-82), APC (Cat: 17-0801-82) or FITC (Cat: 11-0801-82) conjugated anti mouse CD80 antibodies, FITC (Cat: 11-0862-82) or PE (Cat: 12-0862-82) conjugated anti mouse CD86 antibodies, APC conjugated anti mouse CD40 antibody (Cat: 17-0401-82) and PE conjugated anti

mouse B7H1 antibody (Cat: 12-5982-82) were all purchased from eBioscience. All of these fluorescent conjugated antibodies were used for flow cytometry. BODIPY lipid dye 493/503 (Cat: D3922) and HCS lipidTOX red dye (Cat: H34476) were obtained from Invitrogen. These dyes were used for flow cytometry and confocal microscopy. The antibody used for confocal microscopy - un-conjugated anti mouse SIINFEKL-H2Kb complex antibody (Clone: 25-D1.16, Cat: 14-5743-82) was purchased from eBioscience. The antibodies for detection different cellular compartments included EEA1 antibody (marker for early endosome, Cat: ab2900), Giantin antibody (marker for Golgi complex, Cat: ab24586), LAMP2 antibody (marker for lysosome, Cat: ab25339) and calnexin antibody (marker for ER, Cat: ab10286) were obtained from Abcam. ERGIC-53/p58 antibody (marker for ER-Golgi intermediate compartment, Cat: E1031) and Rab5a antibody (marker for early endosome, Cat: NBP1-20255) were purchased from Sigma and Novus Biologicals, respectively. Both Alexa Fluor® 488 conjugated anti-rabbit (Cat: A-11034) or anti-rat (Cat: A-11006) and Alexa Fluor® 594 conjugated anti-rabbit (Cat: A-11037) or anti-rat (Cat: A-11007) secondary antibodies were obtained from Invitrogen.

Preparation of tumor explant supernatant (TES)

TES were prepared from excised non-ulcerated tumors approximately 1.5 cm in diameter. Tumor tissues were bathed in 70% isopropanol for 30 seconds and then transferred to a Petri dish. Tumors were minced into pieces <3mm in diameter and digested in 2mg/mL collagenase Type D/IV at 37°C for one hour. The digested tissue pieces were then pressed through a 70μm mesh screen to create a single cell suspension. Cells were washed with PBS and resuspended in RPMI 1640 supplemented with 20 mM N-2-hydroxyl piperazine-N'-2-ethanesulfonic acid, 2 mM L-glutamine, 200 U/mL penicillin plus 50 μg/mL streptomycin, and 10% FBS. Cells were cultured overnight at 10^7cells/mL and the cell free supernatant were collected and kept at −80°C.

Analysis of cell phenotype by flow cytometry

Cell surface labeling was performed on ice for 20 min and analyzed by a FACSCalibur or LSRII flow cytometer and CellQuest program. For lipid staining, cells were re-suspended in 500uL of Bodipy 493/503 at 0.5 μg/mL in PBS. Cells were stained for 15 min at room temperature, then washed once with PBS, and re-suspended in PBS-DAPI for flow cytometry analysis. At least 10,000 cells were collected for subsequent analysis.

Measurement of activity of protease

DCs were lysed in non-ionic lysis buffer (10mM Tris, PH 7.8; 1% Nonidet P-40, 0.15M Nacl, 1mM EDTA-Na). The cell lysates were centrifugated at 19000 g for 10min at 4°C. 5μg lysate in 100μl substrate buffer (20mM HEPES, PH 8.2, 0.5mM EDTA-Na, 1% DMSO, 5mM ATP) and 1.3μl substrate (stock: 10mmol/L) in 100μl substrate buffer/well were mixed together. After a 30min incubation at 37 degrees, fluorescence (excitation, 380nm; emission, 460nm) was measured using a SpectrafluoPlus 96-well plate reader. The following substrates were used for detection: Z-LLE-AMC (Cat: ZW9345-0005) for caspase; BOC-LRR-AMC (Cat: BW8515-0005) for trypsin; Z-GGL-AMC (Cat: ZW8505-0005) for chymotrypsin; and Ac-KQKLR-AMC (Cat: 61859) for cathepsin-S. Ac-KQKLR-AMC

substrate was purchased from Anasepc, while all other substrates were purchased from Biomol.

Generation and isolation of dendritic cells

Mouse DCs were generated from bone marrow progenitor by a 3-day culture with 10 ng/mL GM-CSF (28). On day 3, medium was replaced with the one containing 20% v/v TES and the cells were cultured for an additional 48 hr. Cells were labeled with biotinylated CD11c antibody (BD Biosciences, San Jose, CA) followed by incubation with magnetic beads, coupled to streptavidin and positive selection on magnetic column according to the manufacturer's protocol (Miltenyi Biotec). In some experiments DCs were generated with 20 ng/mL GM-CSF and 10 ng/mL IL-4 for 5 days. At that time $CD11c^+$ DCs were isolated using magnetic beads and incubated with 20% v/v TES for additional 48 hours. DCs were also directly isolated from mouse spleen, using the same method.

Human DCs were generated from mononuclear cells, isolated from donors' buffy coat blood by ficoll gradient centrifugation. Cells were cultured for 3 days with 40 ng/ml rhGM-CSF and 20 ng/ml IL-4. On day 3, media was replaced and 20% tumor conditioned media, derived from SK-MEL melanoma cell lines. 48 hours later, the non-adherent and loosely adherent cells were collected.

Functional assays

DCs were loaded for 24 h with 100μg/ml OVA or 5 μg/ml long peptides. Before adding to T cells, DCs were irradiated with 20 Gy. T cells were isolated using mouse T cell enrichment columns (R&D Systems). T cells were then plated at 0.2×10^5 T cells per well. DCs and T cells were mixed at different ratios. In experiments with loading of short peptide, 0.1 μg/mL of SIINFEKL was added into the media. Cells were incubated for 72 h. ^{3}[H]-thymidine was then added at 1μCi per 200uL of cells per well for an additional 18 hours of incubation, followed by cell harvesting and a radioactivity count on liquid scintillation counter.

Confocal microscopy

Cells were fixed and permeabilized with Fixation & Permeabilization Buffers (BD) for 20 min at 4°C, washed with PBS, and then blocked with PBS containing 1% FBS for 1h. Cells were incubated with different antibodies overnight at 4°C and hen stained with HCS LipidTOX red lipid stain or BODIPY, to detect lipid bodies for 30 min at 4°C. The cells were imaged with a Leica TCS SP5 laser scanning confocal microscope through a 63X/ 1.40NA Plan Apochromat oil immersion objective lens (Leica Microsystems, Germany). 405nm and 555nm diode lasers lines were applied to excite the samples. An acousto-optical beam splitter (AOBS) was used to collect peak emission photons, sequentially, to minimize crosstalk between fluorochromes.

Protein and peptide liquid chromatography-multiple reaction monitoring mass spectrometry

Cells ($n = 10^5$) were lysed in aqueous 8M urea/100mM ammonium bicarbonate buffer on ice. After lysis, the cell supernatants are clarified by centrifugation and decanted. Lysates were loaded for SDS-PAGE separation (Criterion XT 4-12%) and visualized with colloidal

Coomassie Brilliant Blue G-250 (Bio-Rad, Hercules, CA). Gel regions, determined by comparison with ovalbumin standards, were excised. Proteins were reduced, alkylated, and digested in-gel overnight digestion at 37°C with sequencing grade trypsin (Promega, Madison, WI). The resulting tryptic peptides were concentrated by vacuum centrifugation and resuspended in 2% acetonitrile, with 0.1% formic acid for mass analysis. A digest of ovalbumin standard protein (Sigma, St. Louis, MO) was used for assay development to select peptides between 7 and 25 amino acids in length, for both specificity and sensitivity of detection. Liquid chromatography-multiple reaction monitoring mass spectrometry was performed, as previously described (29).

Liquid chromatography and mass-spectral analysis of lipids

Lipids were extracted by Folch procedure (Folch et al., 1957) with slight modifications, under nitrogen atmosphere, at all steps. LC/ESI-MS analysis was performed on a Dionex HPLC system (utilizing the Chromeleon software), consisting of a Dionex UltiMate 3000 mobile phase pump, equipped with an UltiMate 3000 degassing unit and UltiMate 3000 autosampler (sampler chamber temperature was set at 4°C). The Dionex HPLC system was coupled to a LXQ^{TM} ion trap mass spectrometer or to a hybrid quadrupole-orbitrap mass spectrometer, Q-Exactive (ThermoFisher, Inc., San Jose, CA) with the Xcalibur operating system. The instrument was operated in both the negative and positive ion modes (at a voltage differential of –3.5-5.0 kV, source temperature was maintained at 150°C). For phospholipid (PL) MS analysis, spectra were acquired in negative ion mode using a full range zoom (200-1600 m/z) or ultra-zoom (SIM) scans. Tandem mass spectrometry (MS/MS analysis) of individual PL species was used to determine the fatty acid composition. Spectra of free fatty acids (FFA) were also obtained in negative ion mode. For triglycerides (TAG) MS analysis, spectra were acquired in positive ion mode using range zoom (600 - 1200 m/z). TAG cations were formed through molecular ammonium adduction $(TAG+NH_4)^+$. MS^n analysis was carried out with relative collision energy, ranged from 20-40%, with activation q value at 0.25 for collision-induced dissociation (CID), and q value at 0.7 for pulsed-Q dissocation (PQD) technique. The spectra of cholesterol esters (CE) were also acquired in positive ion mode on a hybrid quadrupole-orbitrap mass spectrometer (Q-Exactive, ThermoFisher, Inc., San Jose, CA).

Statistical Analysis

Statistical analysis was performed using unpaired 2-tailed Student t-test with significance determined at $p<0.05$.

Results

Tumor-derived factors inhibit antigen cross-presentation by DCs

To evaluate the effect of TDF on the ability of differentiated DCs to present antigens, DCs were generated *in vitro* from bone marrow (BM) progenitors in culture with GM-CSF for 3 days. After that time, tumor explant supernatants (TES), from different tumors (EL-4 lymphoma, MC38 colon carcinoma, and CT-26 colon carcinoma), were added for an additional 48 h. Under these conditions, TES did not affect the expression of MHC-I or MHC class II molecules, and caused a slight increase in the expression of co-stimulatory

molecules on DCs (Fig. S1A). Analysis of the expression of markers specific for different myeloid cells (CD11c, CD11b, F4/80, Gr-1) showed that under these conditions TES did not affect the phenotype of differentiated DCs (Fig. S1B). Little differences were observed in the effect of LPS on DC activation (Fig. S1C). After TES treatment, the DCs were loaded with an H-2K^b binding peptide (SIINFEKL) and no defect in their ability to stimulate peptide-specific OT-1 transgenic CD8$^+$ T cells was observed (Fig. 1A). The expression of SIINFEKL/H-2K^b complexes (pMHC) was evaluated by flow cytometry, using the 25-D1.16 antibody, which specifically recognizes OVA derived peptide SIINFEKL bound to H2-Kb of MHC I. The results showed that TES treatment of DCs did not significantly affect the cell surface expression of pMHC, generated by the direct loading of MHC-I with exogenous peptide (Fig. 1B). To assess the effect of TES on antigen cross-presentation, DCs were loaded with ovalbumin protein (OVA), during the last 24 h of culture, and then used for stimulating OT-1 T cells and for the presence of pMHC on the surface of DCs. TES, from all tested tumors, significantly ($p<0.01$) reduced the ability of DCs to stimulate peptide-specific OT-1 T cells (Fig. 1C) and the expression of pMHC on DCs (Fig. 1D). To confirm these observations, we used a long OVA-peptide construct (Pam2-KMFVESIINFEKL) that cannot bind directly to H2K^b; but is very effective in generating pMHC and stimulating CD8 T cell responses (E. Celis, unpublished data). Loading of DCs with Pam2-KMFVESIINFEKL generated a higher density of pMHC, than loading of DCs with OVA protein, which allowed for better visualization of these complexes by microscopy. Treatment of DCs with TES resulted in a substantial decrease of pMHC on the DC surface (Fig. 1E, F). Similar results were obtained using DCs differentiated from BM progenitors with GM-CSF and IL-4 for 5 days (Fig. S2A,B). To confirm inhibition of cross-presentation in a different experimental system, we used another long peptide, (Pam)2-KMFV-KVPRNQDWL, which contains a CD8 T cell epitope from the melanoma associated gp100 protein. Peptide-epitope specific pmel-1 transgenic CD8$^+$ T cells, that recognize the minimal gp100 epitope KVPRNQDWL, were used as responders (30). Similar to the results obtained with OVA, TES inhibited the cross-presentation of the antigen derived from the gp100 long peptide (Fig. 1G).

Next, we asked whether the above-described defects were specifically associated with the exogenous cross-presentation pathway, or would also be observed with the presentation of endogenous antigens. To address this question, we used OVA transgenic mice (OVA-Tg) with a constitutive expression of OVA. Treatment of DCs, generated from these mice, with TES did not affect their ability to stimulate OT-1 T cells (Fig. 1H) and did not decrease pMHC expression on these DCs (Fig. 1I). It was possible that in OVA-Tg DCs pMHC, formed prior to exposure to TES, were still present on the surface of DCs, thus negating the possible effect of TES on *de novo* antigen processing. To address this concern, we stripped peptides from MHC-I on DC surface, before TES application, using a mild acid treatment (Fig. 1J). Under these conditions, TES still did not affect the formation of new surface pMHC on DCs (Fig. 1K). It was possible that DCs in OVA-Tg mice present greater levels of OVA due to a constitutive OVA expression, which could compensate for the effect of TES. We have compared, side-by-side, during the same experiment, the expression of pMHC in DCs loaded with OVA-derived peptide (SIINFEKL) and isolated from OVA-Tg mice. OVA-Tg DCs had lower expression of pMHC than peptide-loaded DCs (Fig. S2C,D). To

confirm the inhibitory effect of tumor derived factors on DC cross presentation, we cultured DCs with supernatant from splenocytes (SES) prepared exactly the same way as TES. SES did not affect DC cross presentation, whereas TES caused profound inhibitory effect in DC loaded with long peptide (Fig. S2C). Thus, taken together these data indicate that TES does not affect the presentation of antigens derived from endogenous proteins and that the effects seem to be circumscribed to the cross-presentation pathway.

We proceeded to evaluate the ability of DCs to process antigens and express pMHC *in vivo*. EL-4 tumors were established in wild-type (WT) and OVA-Tg mice. Spleens were isolated and the pMHC expression was evaluated in $CD11c^{+}IA^{b+}$ total population of DCs and in $CD8^{+}$ subset known to be primarily involved in cross presentation. DCs isolated from TB mice and loaded with long OVA-derived peptide (SIINFEKL) showed significantly reduced presentation of pMHC on the surface (Fig. 2A). In contrast, no decrease in pMHC expression was found in DCs isolated from TB OVA-Tg mice (Fig. 2B). These data support the conclusion that DCs in TB hosts are not able to effectively cross-present exogenous antigens but continue to be effective in processing and presenting endogenous antigens.

Mechanisms of inhibition of cross-presentation in cancer

We had previously observed an accumulation of lipids in DCs, from cancer patients and TB mice, and the association of this accumulation to defects in DC function (27). Therefore, we investigated the possible role of lipids in the defective antigen cross-presentation by DCs in cancer. As expected, a two-day exposure of DCs to TES caused the accumulation of lipids in DCs (Fig. 3A). DCs, treated with TES and loaded with OVA, were gated based on the level of lipids: cells with normal lipid level (LN) and cells with high lipid content (LH). Although no differences were observed in the overall $H\text{-}2K^{b}$ expression between LN and LH DCs, the LN DCs had a substantially higher expression level of pMHC as compared to the LH DCs (Fig. 3B). Similar results were obtained when DCs were loaded with OVA-derived long peptide and exposed to TES from different tumors (Fig. 3C). There was some overlap in pMHC expression between DCs with control and high lipid levels because only 50-60% of TES treated DCs had increased lipid level.

To further assess the possible involvement of lipids in the decreased generation of pMHC via cross-presentation, we used DCs deficient for the scavenger receptor CD204 (Msr1). This receptor was previously found to be primarily responsible for lipid accumulation in DCs in cancer (27). CD204 deficient DCs were generated from bone marrow of $Msr1^{-/-}$ mice and cultured with TES and OVA, as described above. In contrast to wild-type DCs (Fig. 1), TES did not affect the ability of CD204 deficient DCs to stimulate OT-1 T cell proliferation (Fig. 3D) or to express pMHC (Fig. 3E), indicating that lipid accumulation may be directly involved in the defective cross-presentation in DCs in cancer.

Accumulation of oxidized lipids in DCs

Treatment of DCs with TES caused an accumulation of enlarged lipid bodies (LB) in DCs that were easily observed inside the cells (Fig. 4A, red fluorescence). The proportion of DC with enlarged LB has been calculated by counting 100 cells. It increased from 9.2% in control to 43.5% in DCs treated with TES. We tested the possibility that LB co-localized

with the cellular compartments involved in antigen processing and the formation of pMHC and, thus, might interfere with this process. However, no co-localization of LB with lysosomes (Fig. 4A), trans-Golgi network (Fig. 4B), early endosomes (Fig. 4C), or ER (Fig. 4D) was found. These data suggests that enlarged LB in DCs unlikely to cause a direct physical disruption of antigen processing.

In a previous study, we observed an accumulation of triglycerides (TAGs) and free fatty acids (FFAs) in DCs from TB mice treated with TES via CD204 receptor (27). However, it is known that TAGs are not directly taken-up by DCs, but are synthesized inside the cells from fatty acids (FAs) and scavenger receptor A (CD204) binds primarily modified lipoproteins (31). To better understand the nature of lipid accumulation in DCs that affects antigen cross-presentation, we used liquid chromatography/mass-spectrometry to quantitatively characterize different types of lipids and their oxidation products. In control DCs, most of FAs were represented by mono- and polyunsaturated FA (PUFA), with $C_{18:2}$ linoleic acid (LA) being the most abundant PUFA (Fig. 4E). In the presence of TES, DCs accumulate large amounts of PUFA, primarily LA (Fig. 4F). Since unsaturated FFAs are highly susceptible to oxidation, we evaluated the oxidative status of lipids. DCs isolated from spleens of naïve mice contained very little oxidized LA (oxLA); whereas, DCs from TB mice had a markedly higher concentration of oxLA (Fig. 4G). Similar results were obtained with oxidized arachidonic acid (AA), although its level in DCs was substantially lower than that of oxLA. No differences between naïve and TB mice were seen in the levels of oxLA or oxAA in sera. (Fig. 4G). Similarly, DCs cultured without TES contained a practically undetectable level oxLA; whereas, DCs cultured with TES had a dramatically higher amount of oxLA (Fig. 4H). A dramatic accumulation of mono-oxygenated TAGs was seen in DCs treated with TES (Fig. 4I). This was associated with a large increase in the presence of oxidatively truncated TAGs (TAGs that were oxidized with subsequent shortening of the oxygenated FA residues) (Fig. 4J). Culture of DCs with TES also resulted in the accumulation of oxidized cholesterol esters (CEs) (Fig. 4K). No detectable amounts of oxidized phospholipids were observed in different classes of DC phospholipids from either TB animals or DC cultured in the presence of TES (**data not shown**).Typical fragmentation analysis of oxygenated LA species in oxTAGs in DCs is shown in Fig. S3.

The proportion of oxLA among total LA was substantially increased in DCs from TB mice as compared with control DCs. In control DCs, the content of oxidized free LA constituted ~0.2 mol%, whereas in DC's from TB mice it was 2.5 mol%. TAGs containing LA-residues underwent massive oxidative modification in DC from TB mice as compared to naïve animals. For example, the content of oxTAGs at m/z 920 corresponding to oxLA molecular species $C_{18:2}/C_{18:2+3O}/C_{16:0}$ in DC from tumor-bearing mice was 59.3 ± 3.8 vs 1.2 ± 0.1 pmol/10^6 cells in control. Thus, disproportionally higher accumulation of oxidation products vs. increase of the respective neutral lipids was observed in tumor-bearing mice vs naïve animals.

Human DCs, cultured with tumor cell condition medium (TCM), had higher lipid levels than control DCs (Fig. 5A). The predominant type of FFA observed in DCs, generated with TCM, was poorly oxidizable mono-unsaturated $C_{18:1}$ oleic FA (Fig. 5B). However, the concentration of oxLA in these cells was more than 2-fold higher than in DCs cultured in

CM (Fig. 5C). Although the total amount CEs showed no difference between DCs cultured with and without TCM (Fig. 5D), DCs exposed to TCM had a dramatically higher presence of oxCE (Fig. 5E). DCs cultured with TCM had a modestly higher amount of TAGs than DCs cultured without TCM (Fig. 5F). In contrast, TCM caused a substantial accumulation of oxTAG in DCs (Fig. 5G). The detailed structural analysis of oxidized lipids in human DCs is provided in Fig. S3. Taken together, these data indicate that DCs, in the presence of TDF, have a substantial accumulation of oxFA; which apparently incorporated into TAG and CE, generating an increased amount of different oxidized lipid species.

The effect of intracellular oxidized lipids on cross-presentation

In view of the above we next asked whether the accumulation of non-oxidized or oxidized lipids in DCs could have an effect on antigen cross-presentation. Based on the fact that oxLA was the most abundant FA accumulated in DCs in TB mice, we assessed whether the defect in cross-presentation could be reproduced by loading control DCs with LA and its subsequent intracellular oxidation. To induce intracellular peroxidation of neutral lipids, we used a lipophilic peroxyl radical initiator, azobis-(2,4-dimethylvaleronitrile) (AMVN), which partitions into hydrophobic phases (31). AMVN decomposes in lipids at a constant rate to yield carbon-centered alkyl radicals, which react with molecular oxygen to generate reactive peroxyl radicals leading to lipid peroxidation (32). DCs were loaded for 24 h with LA in serum-free medium, treated with AMVN for 2 h, washed, and then used in experiments. Loading of DCs with LA or in combination with AMVN resulted in an accumulation of large LB, similar to the effect of TES (Fig. 6A). At a concentration of 0.2-0.5 mM, AMVN did not affect DC viability or expression of MHC-I, MHC-II or co-stimulatory molecules (Fig. S4A, B). On the other hand, AMVN induced oxidation of LA in DCs (Fig. 6B). In addition to oxLA, we also observed accumulation of oxTAGs and oxCE in DCs loaded with LA and treated with AMVN (Fig. 6C, D). In contrast to robust AMVN-driven accumulation of peroxidation products in major neutral lipid components of LBs (peroxidized species of TAGs, FFA and cholesterol esters were increased up to 244.3 $\pm$ 7.5; 74.8 $\pm$ 12.4 and 1.2 $\pm$ 0.2 pmol/10^6 cells, respectively) only minor peroxidation of membrane phospholipids was detected **(**9.2 $\pm$ 1.8 pmol/10^6 cells) which constitutes ~3% of the total increase in the content of oxidized lipids). Thus, these experimental conditions recapitulated accumulation of ox-lipids in DCs observed on DCs exposed to TES or TCM and were used in further experiments.

After loading with LA, with or without subsequent treatment with AMVN, DCs were incubated overnight with OVA and then used for stimulation of OT-1 T cells. DCs, treated with LA or AMVN alone, showed no defect in antigen cross-presentation function; whereas, a combination of AMVN and LA significantly reduced the ability of the DCs to stimulate antigen-specific T cells (Fig. 6E). In contrast, if DCs were directly loaded with SIINFEKL peptide, the combination of AMVN and LA did not affect DC stimulation of OT-1 T cells (Fig. 6F). Treatment of DCs with LA alone did not affect the pMHC surface expression after loading of the cells with long OVA peptide while AMVN by itself caused a small decrease in the levels of surface pMHC (Fig. 6G). In contrast, the combination of AMVN and LA resulted in a more than 2-fold decrease of pMHC surface expression (Fig. 6G), confirming that the accumulation of ox-lipids in DCs specifically inhibits antigen cross-presentation but

does not affect DC function if the peptide is directly loaded onto the MHC-I on the surface. To confirm these observations in a different experimental system, we loaded DCs with long peptide derived from gp100 protein and used pmel-1 T cells as responders. The combination of LA and AMVN, but not each of them separately, significantly ($p<0.05$) inhibited the cross-presentation function of the DCs (Fig. 6H). To verify the specific role of lipid oxidation in defective cross-presentation in our experimental system, DCs were treated with a higher concentration of AMVN (0.5 mM). At this dose, AMVN directly inhibited the ability of OVA-loaded DCs to stimulate OT-1 T cells without need to pre-load DCs with LA (Fig. 7A). To block lipid peroxidation, we pre-treated cells with alpha-tocopherol (vitamin E) which is known to partition into hydrophobic phases of lipid structures and has been shown to effectively inhibit lipid peroxidation in biomembranes and lipoproteins (33). Tocopherol abrogated the inhibitory effect of AMVN on cross-presentation of OVA to T cells (Fig. 7A); and abrogated the inhibitory effect of AMVN on the expression of pMHC, after DC loading with either OVA or long OVA-derived peptide (Fig. 7B). The negative effect of AMVN on surface pMHC levels affected only cross-presentation, since it was not observed in DCs obtained from OVA-Tg mice (Fig. 7C). Likewise, treatment of DCs with AMVN inhibited the stimulation of OT-1 T cells by DCs loaded with OVA, but did not affect DCs from OVA-Tg mice (Fig. 7D). Thus, ox-lipids can directly inhibit cross-presentation in DCs without affecting the presentation of endogenous antigen.

Mechanism of inhibition of cross-presentation by oxidized lipids

The endogenous pathway of presentation invariably depends on proteasomes; whereas, the pathway of cross-presentation (cytosolic or vacuolar) depends on the type of antigen and the mechanism of its uptake (12, 34). In our experiments, inhibition of proteasomes with lactacystin almost completely abrogated the surface expression of pMHC in DCs isolated from OVA-Tg mice (Fig. 8A). In contrast, lactacystin had little effect on cross-presentation OVA by DCs (Fig. 8A,B) and a modest effect on cross-presentation of long OVA-derived peptide (Fig. 8A), suggesting that a vacuolar mechanism could be the main pathway involved in cross-presentation under these circumstances.

IFN-γ is known to up-regulate MHC-I expression and increase cross-presentation in DCs. We assessed whether pre-treatment of DCs with IFN-γ would abrogate the inhibitory effect of TES on cross-presentation. As expected, in DCs cultured in control medium, IFN-γ caused a marked up-regulation of overall H-2K^b and more than a two-fold increase in the expression of pMHC, after DC loading with long OVA peptide (Fig. S4C). IFN-γ substantially up-regulated the expression of H-2K^b on DCs cultured with TES from three different tumors (Fig. 8C, top panels). However, IFNγ did not completely overcome the block in pMHC expression(Fig. 8C, bottom panels). Treatment of DCs with IFN-γ did not rescue inhibited by TES DC ability to stimulate OT-1 T cell proliferation after cross-presentation of OVA protein (Fig. 8D). We also tested the effect of IFN-γ on cross-presentation of DCs loaded with LA and treated with AMVN. Similar to the effect observed in the presence of TES, IFN-γ up-regulated the H-2K^b expression, but failed to abrogate the defect in pMHC expression (Fig. 8E). Despite the presence of a small population of DCs with increased expression of pMHC, we did not find an improvement in the ability of DCs

to stimulate antigen-specific T cells after cross-presentation of OVA-derived long peptide (Fig. 8F).

Discussion

Here, we report for the first time that oxidized lipids inhibit cross-presentation in DCs. This may have an implication on therapeutic efforts in patients with low tumor burden, who are considered optimal candidates for cancer vaccines. Accumulation of lipids in DCs, from TB hosts, is mediated via up-regulation of scavenger receptor (Msr1 or CD204). This receptor binds various acetylated and oxidized lipids, including low-density lipoproteins (LDLs) (35). Msr1–deficient DCs showed a more effective antigen-presenting capability, as compared with wild-type cells, but this was primarily linked with their more mature phenotype (36). In the absence of CD204 (in *Msr1*$^{-/-}$ mice), TDF failed to inhibit the antigen cross-presentation function in DCs, supporting the possible role of a lipid uptake in the negative effects of TDF on DCs. Extracellular lipids may affect DC function via various receptor-mediated mechanisms (37, 38) (39, 40). However, our data indicated that the effect of lipids on cross-presentation was primarily intracellular. When DCs treated with TDF were separated based on their level of intracellular lipids, the defect in cross-presentation was associated only with high lipid laden DCs. We previously have shown that although TES obtained from different tumor cell lines had variable levels of TAGs, they caused comparable up-regulation of lipids in DCs (27). It is known that TAGs are not directly taken-up by DCs, but are synthesized inside the cells from fatty acids (FAs). CD204 binds modified primarily oxidized lipoproteins (35).

Small lipid bodies (LBs) are present in all DCs and have been implicated in cross-presentation via interaction with Irgm3, an IFN-related GTPase (IRG). Irgm3 is required for IFN-γ-induced efficient cross-presentation (24). Using high-resolution confocal microscopy, van Manen et al. have demonstrated the transient association of LBs with latex bead-containing phagosomes in neutrophils and macrophages (41). If LBs are important for cross-presentation and could be transiently associated with phagosomes, then it was conceivable that large LBs could disrupt cross-presentation. However, our data argue against this possibility, since we could not detect co-localization of large LBs with any cellular compartment associated with cross-presentation or with pMHC. Treatment of DCs with IFN-γ did not rescue the defect of cross-presentation caused by TDF, despite the substantial up-regulation of MHC-I. Loading of DCs with LA, that resulted in formation of large LBs, did not cause the defect in cross-presentation by DCs. Thus, it appears that the mere accumulation of lipids in DCs is not sufficient to affect cross-presentation.

Our data demonstrated a substantial accumulation of different classes of neutral ox-lipids in DCs in TB hosts, which is consistent with the important role of CD204 in this process (42). To directly test the hypothesis that ox-lipids are involved in regulation of cross-presentation, we could not use a treatment with extracellular oxidized lipoproteins or lipids. Oxidized and non-oxidized lipids and lipoproteins differ in the nature of the receptors they bind and signaling they cause, as well as in the kinetic of their uptake by the cells (43). DCs are lacking the machinery for lipid peroxidation and TDF did not cause the up-regulation of myeloperoxidase or ROS needed for this process. Therefore, in our model experiments, we

used a LA and lipophilic generator of peroxyl radicals, AMVN. Our data directly implicated intracellular ox-lipids in the inhibition of cross-presentation in DCs.

Why do oxidized lipids affect only cross-presentation and not presentation of endogenous antigens? In contrast to endogenous presentation, which involves the proteasomal degradation of proteins, the transfer of peptides to the ER by TAP, and the formation of pMHC in the ER with the subsequent transport to the membrane (44); these components are not essential for the vacuolar pathway in antigen cross-presentation (45). This pathway largely involves the recycling of MHC-I from the surface and formation of new pMHC in endosomes and lysosomes via peptide exchange. The cytoplasmic domain of MHC-I can direct the protein to both the endosomal and lysosomal compartments of DCs, where loading of peptides derived from exogenous proteins can occur (46, 47). In addition to recycling MHC-I, transport of MHC-I, from ER to the endocytic compartment, has also been demonstrated (48, 49).

We propose the concept of disrupted DC antigen cross-presentation in cancer. Under physiological conditions, DCs, in contrast to neutrophils and macrophages, produce and accumulate very low levels of peroxidized lipids. In TB hosts, TDF induce the up-regulation of Msr1 (27), which facilitates an uptake of peroxidized lipids present in plasma or tumor cell conditioned medium. Inside DCs, oxidized lipid moiety can be directly trafficked to endosomes and localized in the lysosomal compartment(50). In addition, the accumulation of lipids in DCs manifests in the formation of large LB. The presence and size of LBs is defined by the accumulation of FA-precursors and their esterification into TAGs and CEs – the major constituents of the hydrophobic core of LBs (26). The significant uptake of oxFFAs, in particular oxLA, facilitates its integration into ox-LA-containing TAGs and CEs. The presence of very polar groups in these oxidized lipid species, or oxidatively truncated TAGs causes their translocation and integration into the less hydrophobic surface area of LBs, where they can be further metabolized (eg, hydrolyzed) by the respective hydrolyzing enzymes. These peroxidized lipid species could be located in the close molecular proximity to the contact sites with neighboring organelles, such as lysosomes. As a result of this proximity, the direct transfer of peroxidized lipids from LBs into lysosomes becomes possible. The exact mechanisms and pathways, through which these peroxidized lipids affect the cross presentation process, remain to be elucidated.

Our data describe a novel mechanism of inhibition cross-presentation in DCs, associated with oxidized lipids, which may play an important role in the negative regulation of cross-presentation in cancer and, possibly, in other pathological processes associated with the accumulation of oxidized lipids; and may suggest potential targets for therapeutic regulation of cross-presentation. It is possible that this mechanism may affect recycling of other receptors and thus affect function of the cells.

Supplementary Material

Refer to Web version on PubMed Central for supplementary material.

References

1. Hildner K, Edelson BT, Purtha WE, Diamond M, Matsushita H, Kohyama M, Calderon B, Schraml BU, Unanue ER, Diamond MS, Schreiber RD, Murphy TL, Murphy KM. Batf3 deficiency reveals a critical role for CD8alpha+ dendritic cells in cytotoxic T cell immunity. Science. 2008; 322:1097–1100. [PubMed: 19008445]
2. Knight SC, Iqball S, Roberts MS, Macatonia S, Bedford PA. TRANSFER OF ANTIGEN BETWEEN DENDRITIC CELLS IN THE STIMULATION OF PRIMARY T CELL PROLIFERATION. Eur. J. Immunol. 1998; 28:1636–1644. [PubMed: 9603470]
3. Yewdall AW, Drutman SB, Jinwala F, Bahjat KS, Bhardwaj N. CD8+ T cell priming by dendritic cell vaccines requires antigen transfer to endogenous antigen presenting cells. PloS one. 2010:5–e11144.
4. Gabrilovich DI, Ostrand-Rosenberg S, Bronte V. Coordinated regulation of myeloid cells by tumours. Nat Rev Immunol. 2012; 12:253–268. [PubMed: 22437938]
5. Ascierto PA, Napolitano M, Celentano E, Simeone E, Gentilcore G, Daponte A, Capone M, Caraco C, Calemma R, Beneduce G, Cerrone M, De Rosa V, Palmieri G, Castello G, Kirkwood JM, Marincola FM, Mozzillo N. Regulatory T cell frequency in patients with melanoma with different disease stage and course, and modulating effects of high-dose interferon-alpha 2b treatment. J Transl Med. 2010; 8:76. [PubMed: 20712892]
6. Yigit R, Figdor CG, Zusterzeel PL, Pots JM, Torensma R, Massuger LF. Cytokine analysis as a tool to understand tumour-host interaction in ovarian cancer. Eur J Cancer. 2011; 47:1883–1889. [PubMed: 21514148]
7. Yamagami W, Susumu N, Tanaka H, Hirasawa A, Banno K, Suzuki N, Tsuda H, Tsukazaki K, Aoki D. Immunofluorescence-detected infiltration of CD4+FOXP3+ regulatory T cells is relevant to the prognosis of patients with endometrial cancer. International journal of gynecological cancer : official journal of the International Gynecological Cancer Society. 2011; 21:1628–1634. [PubMed: 21897268]
8. Shen X, Li N, Li H, Zhang T, Wang F, Li Q. Increased prevalence of regulatory T cells in the tumor microenvironment and its correlation with TNM stage of hepatocellular carcinoma. J Cancer Res Clin Oncol. 2010; 136:1745–1754. [PubMed: 20221638]
9. Bevan MJ. Minor H antigens introduced on H-2 different stimulating cells cross-react at the cytotoxic T cell level during in vivo priming. J Immunol. 1976; 117:2233–2238. [PubMed: 825578]
10. Bevan MJ. Cross-priming for a secondary cytotoxic response to minor H antigens with H-2 congenic cells which do not cross-react in the cytotoxic assay. J Exp Med. 1976; 143:1283–1288. [PubMed: 1083422]
11. Burgdorf S, Kurts C. Endocytosis mechanisms and the cell biology of antigen presentation. Curr Opin Immunol. 2008; 20:89–95. [PubMed: 18249105]
12. Joffre OP, Segura E, Savina A, Amigorena S. Cross-presentation by dendritic cells. Nat Rev Immunol. 2012; 12:557–569. [PubMed: 22790179]
13. Alvarez D, Vollmann EH, von Andrian UH. Mechanisms and consequences of dendritic cell migration. Immunity. 2008; 29:325–342. [PubMed: 18799141]
14. McDonnell AM, Prosser AC, van Bruggen I, Robinson BW, Currie AJ. CD8alpha+ DC are not the sole subset cross-presenting cell-associated tumor antigens from a solid tumor. Eur J Immunol. 2010; 40:1617–1627. [PubMed: 20373290]
15. van Mierlo GJ, Boonman ZF, Dumortier HM, den Boer AT, Fransen MF, Nouta J, van der Voort EI, Offringa R, Toes RE, Melief CJ. Activation of dendritic cells that cross-present tumor-derived antigen licenses CD8+ CTL to cause tumor eradication. J Immunol. 2004; 173:6753–6759. [PubMed: 15557168]
16. Gerner MY, Casey KA, Mescher MF. Defective MHC class II presentation by dendritic cells limits CD4 T cell help for antitumor CD8 T cell responses. J Immunol. 2008; 181:155–164. [PubMed: 18566380]
17. Engelhardt JJ, Boldajipour B, Beemiller P, Pandurangi P, Sorensen C, Werb Z, Egeblad M, Krummel MF. Marginating dendritic cells of the tumor microenvironment cross-present tumor

antigens and stably engage tumor-specific T cells. Cancer Cell. 2012; 21:402–417. [PubMed: 22439936]

18. Perrot I, Blanchard D, Freymond N, Isaac S, Guibert B, Pacheco Y, Lebecque S. Dendritic cells infiltrating human non-small cell lung cancer are blocked at immature stage. J Immunol. 2007; 178:2763–2769. [PubMed: 17312119]
19. Gabrilovich DI. The mechanisms and functional significance of tumour-induced dendritic-cell defects. Nat Rev Immunol. 2004; 4:941–952. [PubMed: 15573129]
20. Melief CJ. Cancer immunotherapy by dendritic cells. Immunity. 2008; 29:372–383. [PubMed: 18799145]
21. Preynat-Seauve O, Schuler P, Contassot E, Beermann F, Huard B, French LE. Tumor-infiltrating dendritic cells are potent antigen-presenting cells able to activate T cells and mediate tumor rejection. J Immunol. 2006; 176:61–67. [PubMed: 16365396]
22. Wakim LM, Bevan MJ. Cross-dressed dendritic cells drive memory CD8+ T-cell activation after viral infection. Nature. 2011; 471:629–632. [PubMed: 21455179]
23. Dolan BP, Gibbs KD Jr. Ostrand-Rosenberg S. Dendritic cells cross-dressed with peptide MHC class I complexes prime CD8+ T cells. J Immunol. 2006; 177:6018–6024. [PubMed: 17056526]
24. Bougneres L, Helft J, Tiwari S, Vargas P, Chang BH, Chan L, Campisi L, Lauvau G, Hugues S, Kumar P, Kamphorst AO, Dumenil AM, Nussenzweig M, MacMicking JD, Amigorena S, Guermonprez P. A role for lipid bodies in the cross-presentation of phagocytosed antigens by MHC class I in dendritic cells. Immunity. 2009; 31:232–244. [PubMed: 19699172]
25. Saka HA, Valdivia R. Emerging roles for lipid droplets in immunity and host-pathogen interactions. Annual review of cell and developmental biology. 2012; 28:411–437.
26. Walther TC, Farese RV Jr. Lipid droplets and cellular lipid metabolism. Annu Rev Biochem. 2012; 81:687–714. [PubMed: 22524315]
27. Herber DL, Cao W, Nefedova Y, Novitskiy SV, Nagaraj S, Tyurin VA, Corzo A, Cho HI, Celis E, Lennox B, Knight SC, Padhya T, McCaffrey TV, McCaffrey JC, Antonia S, Fishman M, Ferris RL, Kagan VE, Gabrilovich DI. Lipid accumulation and dendritic cell dysfunction in cancer. Nat Med. 2010; 16:880–886. [PubMed: 20622859]
28. Zhou J, Cheng P, Youn JI, Cotter MJ, Gabrilovich DI. Notch and wingless signaling cooperate in regulation of dendritic cell differentiation. Immunity. 2009; 30:845–859. [PubMed: 19523851]
29. Remily-Wood ER, Liu RZ, Xiang Y, Chen Y, Thomas CE, Rajyaguru N, Kaufman LM, Ochoa JE, Hazlehurst L, Pinilla-Ibarz J, Lancet J, Zhang G, Haura E, Shibata D, Yeatman T, Smalley KS, Dalton WS, Huang E, Scott E, Bloom GC, Eschrich SA, Koomen JM. A database of reaction monitoring mass spectrometry assays for elucidating therapeutic response in cancer. Proteomics. Clinical applications. 2011; 5:383–396. [PubMed: 21656910]
30. Overwijk WW, Tsung A, Irvine KR, Parkhurst MR, Goletz TJ, Tsung K, Carroll MW, Liu C, Moss B, Rosenberg SA, Restifo NP. gp100/pmel 17 is a murine tumor rejection antigen: induction of "self"-reactive, tumoricidal T cells using high-affinity, altered peptide ligand. J Exp Med. 1998; 188:277–286. [PubMed: 9670040]
31. Bieghs V, Verheyen F, van Gorp PJ, Hendrikx T, Wouters K, Lutjohann D, Gijbels MJ, Febbraio M, Binder CJ, Hofker MH, Shiri-Sverdlov R. Internalization of modified lipids by CD36 and SR-A leads to hepatic inflammation and lysosomal cholesterol storage in Kupffer cells. PloS one. 2012; 7:e34378. [PubMed: 22470565]
32. Tyurina YY, Tyurin VA, Shvedova AA, Fabisiak JP, Kagan VE. Peroxidation of phosphatidylserine in mechanisms of apoptotic signaling. Methods Enzymol. 2002; 352:159–174. [PubMed: 12125344]
33. Tsuchiya M, Kagan VE, Freisleben HJ, Manabe M, Packer L. Antioxidant activity of alpha-tocopherol, beta-carotene, and ubiquinol in membranes: cis-parinaric acid-incorporated liposomes. Methods Enzymol. 1994; 234:371–383. [PubMed: 7808309]
34. Burgdorf S, Scholz C, Kautz A, Tampe R, Kurts C. Spatial and mechanistic separation of cross-presentation and endogenous antigen presentation. Nat Immunol. 2008; 9:558–566. [PubMed: 18376402]
35. Platt N, Gordon S. Is the class A macrophage scavenger receptor (SR-A) multifunctional? - The mouse's tale. J Clin Invest. 2001; 108:649–654. [PubMed: 11544267]

36. Wang XY, Facciponte J, Chen X, Subjeck JR, Repasky EA. Scavenger receptor-A negatively regulates antitumor immunity. Cancer Res. 2007; 67:4996–5002. [PubMed: 17510431]
37. Aliberti J, Hieny S, Reis e Sousa C, Serhan CN, Sher A. Lipoxin-mediated inhibition of IL-12 production by DCs: a mechanism for regulation of microbial immunity. Nat Immunol. 2002; 3:76–82. [PubMed: 11743584]
38. Weatherill AR, Lee JY, Zhao L, Lemay DG, Youn HS, Hwang DH. Saturated and polyunsaturated fatty acids reciprocally modulate dendritic cell functions mediated through TLR4. J Immunol. 2005; 174:5390–5397. [PubMed: 15843537]
39. Shamshiev AT, Ampenberger F, Ernst B, Rohrer L, Marsland BJ, Kopf M. Dyslipidemia inhibits Toll-like receptor-induced activation of CD8{alpha}-negative dendritic cells and protective Th1 type immunity. J Exp Med. 2007; 204:441–452. [PubMed: 17296788]
40. Angeli V, Llodra J, Rong JX, Satoh K, Ishii S, Shimizu T, Fisher EA, Randolph GJ. Dyslipidemia associated with atherosclerotic disease systemically alters dendritic cell mobilization. Immunity. 2004; 21:561–574. [PubMed: 15485633]
41. van Manen H-J, Kraan YM, Roos D, Otto C. Single-cell Raman and fluorescence microscopy reveal the association of lipid bodies with phagosomes in leukocytes. PNAS. 2005; 102:10159–10164. [PubMed: 16002471]
42. Tyurin VA, Cao W, Tyurina YY, Gabrilovich DI, Kagan VE. Mass-spectrometric characterization of peroxidized and hydrolyzed lipids in plasma and dendritic cells of tumor-bearing animals. Biochem Biophys Res Commun. 2011; 413:149–153. [PubMed: 21872574]
43. Zaguri R, Verbovetski I, Atallah M, Trahtemberg U, Krispin A, Nahari E, Leitersdorf E, Mevorach D. 'Danger' effect of low-density lipoprotein (LDL) and oxidized LDL on human immature dendritic cells. Clin Exp Immunol. 2007; 149:543–552. [PubMed: 17645766]
44. Jensen PE. Recent advances in antigen processing and presentation. Nat Immunol. 2007; 8:1041–1048. [PubMed: 17878914]
45. Touret N, Paroutis P, Terebiznik M, Harrison RE, Trombetta S, Pypaert M, Chow A, Jiang A, Shaw J, Yip C, Moore HP, van der Wel N, Houben D, Peters PJ, de Chastellier C, Mellman I, Grinstein S. Quantitative and dynamic assessment of the contribution of the ER to phagosome formation. Cell. 2005; 123:157–170. [PubMed: 16213220]
46. Basha G, Lizee G, Reinicke AT, Seipp RP, Omilusik KD, Jefferies WA. MHC class I endosomal and lysosomal trafficking coincides with exogenous antigen loading in dendritic cells. PloS one. 2008; 3:e3247. [PubMed: 18802471]
47. Lizee G, Basha G, Tiong J, Julien JP, Tian M, Biron KE, Jefferies WA. Control of dendritic cell cross-presentation by the major histocompatibility complex class I cytoplasmic domain. Nat Immunol. 2003; 4:1065–1073. [PubMed: 14566337]
48. Gagnon E, Duclos S, Rondeau C, Chevet E, Cameron PH, Steele-Mortimer O, Paiement J, Bergeron JJ, Desjardins M. Endoplasmic reticulum-mediated phagocytosis is a mechanism of entry into macrophages. Cell. 2002; 110:119–131. [PubMed: 12151002]
49. Basha G, Omilusik K, Chavez-Steenbock A, Reinicke AT, Lack N, Choi KB, Jefferies WA. A CD74-dependent MHC class I endolysosomal cross-presentation pathway. Nat Immunol. 2012; 13:237–245. [PubMed: 22306692]
50. Al Gadban MM, Smith KJ, Soodavar F, Piansay C, Chassereau C, Twal WO, Klein RL, Virella G, Lopes-Virella MF, Hammad SM. Differential trafficking of oxidized LDL and oxidized LDL immune complexes in macrophages: impact on oxidative stress. PloS one. 2010:5.

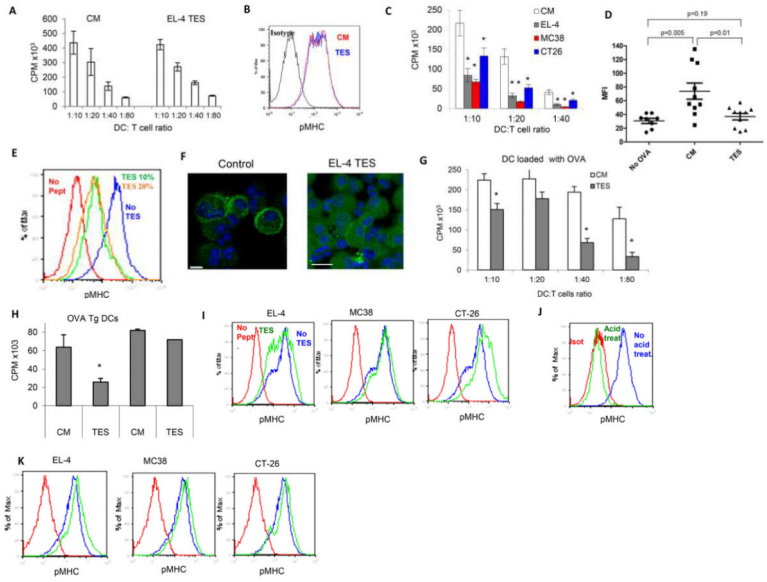

Figure 1. Effect of tumor-derived factors on cross-presentation in DCs

A. Stimulation of OT-1 $CD8^+$ T cell proliferation by $CD11c^+$ DCs cultured with TES from EL-4 tumors for 48 h. Cells were cultured at indicated ratios in the presence of 0.1 μg/ml of control (RAHYNIVTF) or specific (SIINFEKL) peptides. Proliferation was measured in triplicate by ^{3}H-thymidine uptake. Proliferation of T cells, in the presence of control peptide, was less than 1,000 CPM and is not shown. Three experiments, with the same results, were performed. **B.** Expression of pMHC in DCs loaded with SIINFEKL. CM – DCs incubated in complete medium. TES – DCs incubated with EL-4 TES. Three experiments, with the same results, were performed. **C.** Stimulation of OT-1 T cells by DCs, incubated for 2 days in complete medium (CM), or TES and loaded for 24 h with 100 μg/ml OVA. Cell proliferation was measured in triplicate by ^{3}[H]-thymidine uptake. Typical results of 4 performed experiments are shown. **D**. Cumulative results of pMHC expression of DCs surface, after loading of cells with 100 μg/ml OVA. TES were obtained from EL-4 tumors. pMHC expression was measured within gated $CD11c^+$ DCs. **E**. Typical example of TES effect on pMHC expression in DCs loaded with 5 μg/ml long OVA peptide. Three experiments, with the same results, were performed. **F**. pMHC staining of $CD11c^+$ DCs, cultured for 24 h with EL-4 TES, and loaded with long peptide for an additional 24 h. Cells were stained with a 25-d1.16 primary and goat Alexa 488 conjugated anti-mouse secondary antibody. Scale bar = 100 μm. **G**. Effect of TES on the ability of DCs cross-present long gp100 derived peptide. Pmel-1 transgenic T cells were used as responders. Cell proliferation was measured in triplicate by ^{3}[H]-tyhymidine uptake. Two experiments, with the same results, were performed. **H.** Effect of EL-4 TES (48 h incubation) on the presentation of endogenous antigen in OVA-Tg DCs or after loading of wild-type DCs with OVA. OT-1 T-cell proliferation was measured in triplicate. One DCs:OT-1 splenocytes ratio (1:20) is shown. Three experiments, with the same results, were performed. **I**. Effect of TES on presentation of pMHC by OVA-Tg DCs after 48 h incubation. For each TES, at least three experiments, with the same results, were performed. **J**. Effect of mild acid treatment (0.263 M citric acid and 0.123 M disodium phosphate, pH 3.0 for 2 min followed by extensive wash in PBS) on the removal of peptide from MHC class I on OVA-Tg DCs. Two experiments, with the same results, were performed. **K**. The effect of TES on pMHC expression in OVA-Tg DCs after mild acid treatment. For each TES, two experiments, with the same results, were performed. In all experiments, * designates statistically significant ($p<0.05$) differences from control.

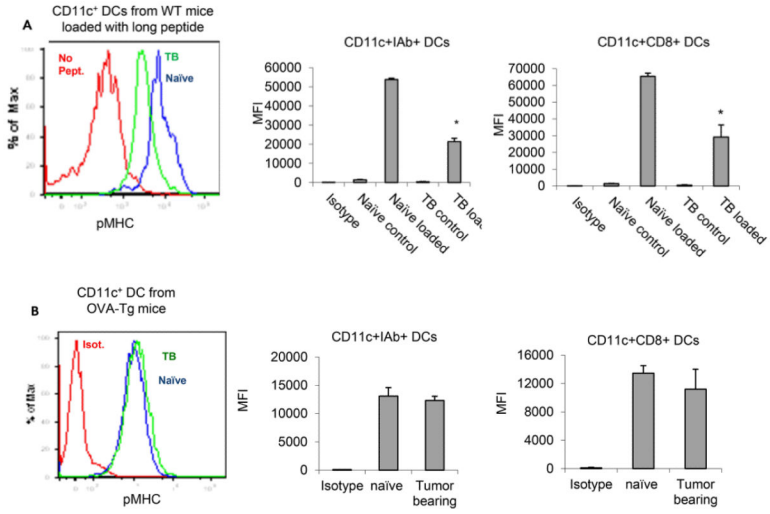

Figure 2. Cross-presentation in DCs isolated from tumorbearing mice

A. Expression of pMHC on the surface of CD11c$^+$ DCs isolated from spleens of naïve or EL-4 TB (tumor ≈ 1cm in diameter) mice and loaded with 5 μg/ml of OVA long peptide. On the left, typical example of staining. On the right, the cumulative results of four experiments in indicated populations of DCs. **B.** Expression of pMHC on the surface of DCs isolated from spleens of naïve or EL-4 TB (tumor ≈ 1cm in diameter) OVA-Tg mice. On the left, typical example of staining. On the right, the cumulative results of four experiments in indicated populations of DCs. In all experiments, * designates statistically significant ($p<0.05$) differences from control.

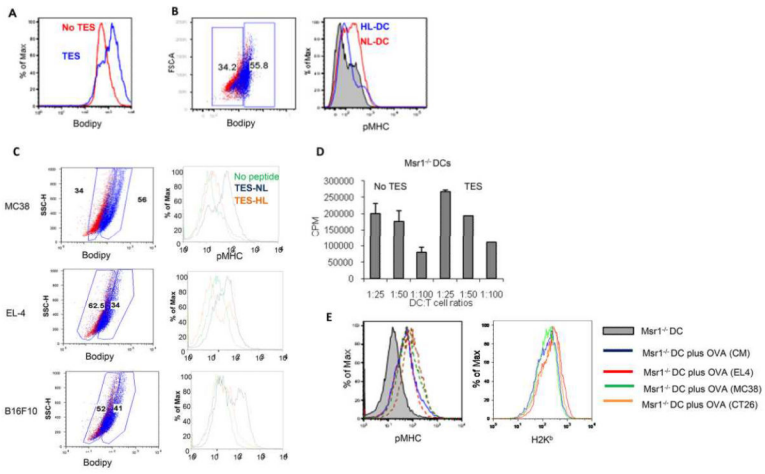

Figure 3. Effect of TES on antigen processing in DCs

A. Typical example of lipid level in gated CD11c^{+} DCs treated with EL-4 TES for 48 h after staining with BODIPY. Seven experiments with similar results were performed. **B**. Cross presentation of antigens by DCs with different levels of lipids. DCs treated with TES and loaded with OVA were stained with BODIPY. Left panel - example of gates set for discriminating DCs with normal lipid levels (NL-DCs) from DCs with high lipid levels (HL-DCs). DCs were considered NL-DCs when their fluorescence overlapped the fluorescence of the control DCs. Control DCs in red; DCs treated with TES in blue. Three experiments, with the same results, were performed. **C.** Cross presentation of long OVA peptide by DCs with different levels of lipids. Left panels show the gate of NL-DCs and HL-DCs and pMHC expression is shown in the right panel. **D**. TES does not affect cross-presentation in CD204 deficient DCs. DCs generated from *Msr1*$^{-/-}$ mice were treated with TES, loaded with OVA, and used for stimulation of OT-1 T cells as described in Fig. 1C. Proliferation of OT-I T cells was measured in triplicate. Typical results of 4 performed experiments are shown. **E.** Typical examples of pMHC (left panel) and H2K^{b} (right panel) expression in CD204 deficient DCs. Grey shaded line - DCs without OVA treatment; blue line - DCs loaded with OVA in control medium (CM); red, green, and orange lines - DCs loaded with OVA and pre-treated with TES from EL-4, MC38, and CT26 tumors, respectively.

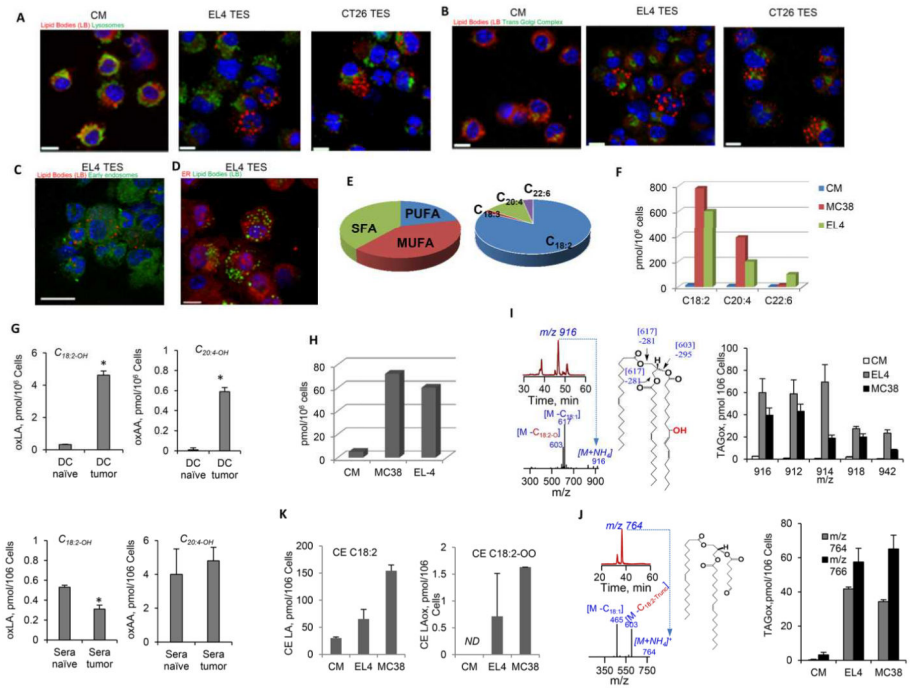

Figure 4. Lipid accumulation in mouse DCs

A-D. Co-localization of LB and cell compartments involved in cross-presentation after 48 h culture of DCs with TES. Lipids were stained with HCS LipidTOX (red fluorescence); lysosomes with LAMP2 antibody (**A**); trans-Golgi complex with giantin antibody (**B**); early endosomes with Rab5a antibody (**C**); ER with calnexin antibody **(D)**. Alexa Fluor® 488 (green fluorescence) labeled secondary antibody, was used in all cases; except for **D,** where Alexa Fluor® 594 (red fluorescence) and BODIOY lipid dye (green fluorescence) were used. Scale bar = 100 μm. Four experiments with the same results were performed. **E**. The proportion of different classes of free FA (left panel) and individual unsaturated FA (right panel) in control DCs; **F.** The presence of different unsaturated FA in DCs. **G**. Oxidized $C_{18:2}$ LA and $C_{20:4}$ AA in spleen DCs and sera from EL-4 TB mice (three mice per group). **H.** The presence oxLA in DCs incubated with TES. **I.** Accumulation of mono-oxygenated TAGs in mouse DCs cultured in the presence of control medium (CM) or EL4, MC38 TES. Typical LC-ESI-MS profiles of TAG with m/z 916 (upper left panel), its MS^2 spectrum (lower left panel) and its suggested structure (middle panel). Right panel - amount of oxTAG 54:6, 54:5, 54:3 and 56:5 at m/z 912, 914, 918 and 942. **J.** Accumulation of truncated oxTAGs in mouse DCs, cultured in the presence of control medium (CM) or EL4, MC38 TES. Typical LC-ESI-MS profile of truncated TAG with m/z 764 (upper left panel), its MS^2 spectrum (lower left panel), and possible structure (middle panel). Fragmentation of the parent ion at m/z 764 $[M+NH_4]^+$ reveals product ions at m/z 603 and 465. The product ion, at m/z 603, was formed by loss of the truncated acyl chain (that corresponded to 7-oxo-heptanoic acid). The product ion, at m/z 465, was formed by loss of oleic acid. Right panel – amount of truncated TAGs. **K.** Content of LA-CE (left panel) and oxLA-CE ($C_{18:2\text{-}2O}$) (right panel) in DCs treated with TES.

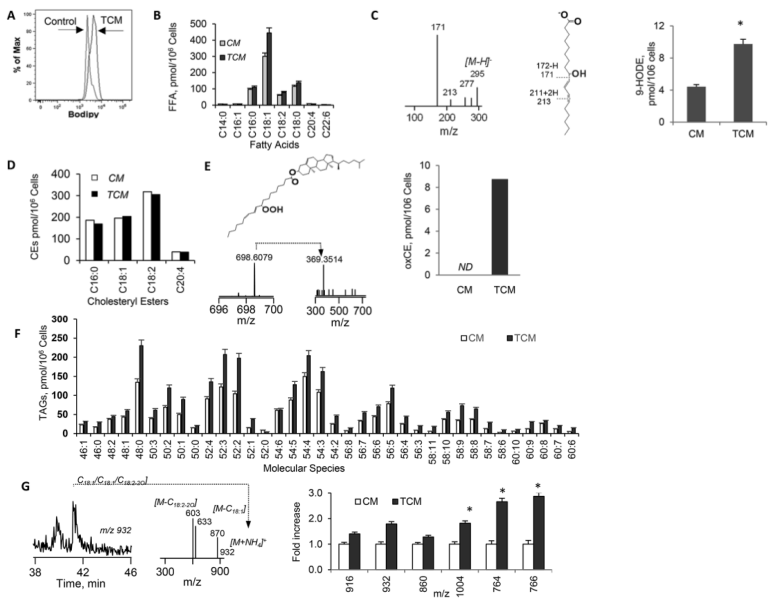

Figure 5. Accumulation of oxidized lipids in human DCs

A. Total lipids in donor's DCs treated with SK-MEL TCM. Typical example of BODIPY staining. **B.** Major FFAs detected in DCs; **C.** oxLA in DCs. MS^2 spectrum of parent ions at m/z 295 (left panel), its possible structure (middle panel), the amount of oxLA (9-HODE) in DCs (right panel); **D.** Cholesteryl Esters (CE) levels in human DCs cultured with and without TCM; **E.** oxCE in DCs. Possible structure of CE 18:2-OOH (upper left panel); MS1 and MS2 spectra of CE 18:2-OOH (lower left panel); amount of CE 18:2-OOH in DCs (right panel). *ND* - not detected. **F.** Accumulation of individual molecular species of TAGs in DCs. **G.** OxTAGs in DCs. Typical LC-ESI-MS profile (left panel); MS^2 spectrum of TAG at m/z 932 (middle panel); amount of oxTAGs in DCs (right panel). Fold increase over values in DCs cultured in CM are shown. **B-G** Two experiments were performed.

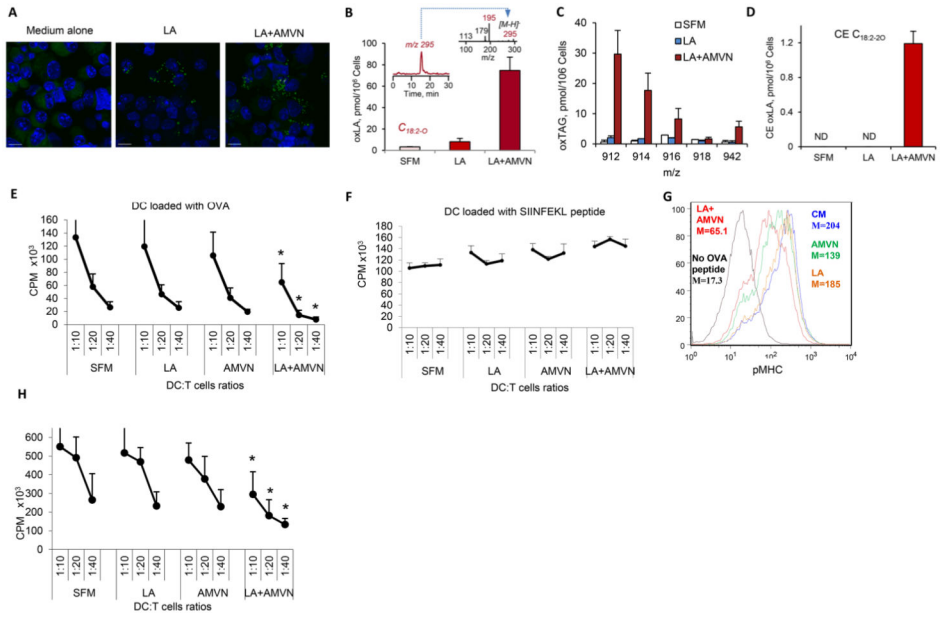

Figure 6. Effect of oxidized LA on cross-presentation by DCs

A. Accumulation of large LB in DCs cultured with LA and LA+AMVN. DCs were cultured for 24 h in serum free medium with 10μg/ml LA and then treated with AMVN (0.2mM) for 2h, prior to washing and loading with OVA (100 μg/ml). Cells were analyzed 18 h later. Staining with BODIPY (scale bar = 100 μm); **B.** Amount of oxLA in the absence and in the presence of AMVN, inset - LC-MS profile and MS2 spectrum**; C.** Contents of major molecular species of oxTAGs containing LA; **D.** Amount of oxCE $C_{18:2\text{-}2O}$ in DCs after loading with LA in the absence and in the presence of AMVN; **E.** Stimulation of OT-1 T cells, by DCs pre-treated with LA and AMVN and loaded with OVA. Experiments were performed in triplicate and repeated twice. **F.** Stimulation of OT-1 T cells, by DCs pre-treated with LA and AMVN and loaded with SIINFEKL peptide. Experiments were performed in triplicate and repeated three times. **G.** pMHC expression in $CD11c^{+}$ DCs, pre-treated with LA and AMVN and loaded with long OVA-derived peptide. Experiments were performed twice. **H.** Stimulation of pmel-1 T cells by DCs, pre-treated with LA and AMVN and loaded with long gp100-derived peptide. Experiments were performed in triplicate and repeated twice.

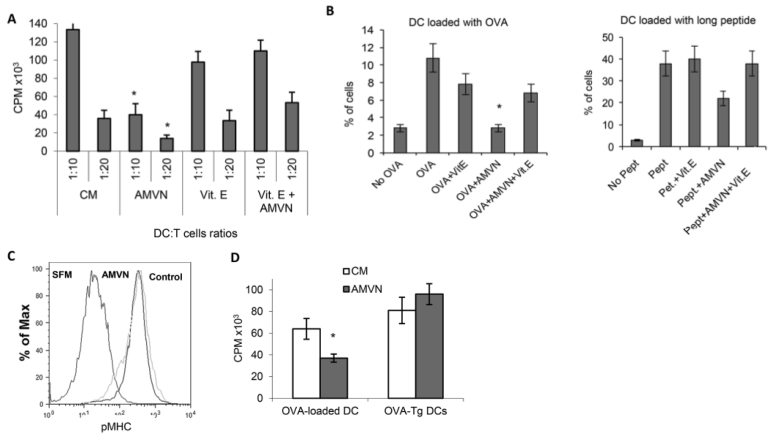

Figure 7. The role of oxidized lipids in cross-presentation

A. The protection effect of vitamin E on cross-presentation. DCs were treated with vitamin E (50μM) for 24 h, followed by 2 h treatment with 0.5 μM AMVN. Cells then were loaded with 100 μg/ml OVA overnight and used for stimulation of OT-1 T cells. Typical results of T-cell proliferation of 4 performed experiments are shown. T cells alone had ^{3}[H]-thymidine uptake of less than 500 CPM. **B**. Percentage of CD11c^{+} DCs expressing pMHC, after the treatment with vitamin E and AMVN, as described above. Left panel - DCs loaded with 100μg/ml OVA; right panel – DCs loaded with 5μg/ml OVA-derived long peptide. Cumulative result of 4 experiments is shown. **C**. pMHC expression on DCs, generated from bone marrow of OVA-Tg mice and treated with 0.5 mM AMVN. Three experiments with the same results were performed. **D.** Proliferation of OT-1 T cells, stimulated with DCs from wild-type mice loaded with OVA and from OVA-Tg mice. DCs were pre-treated with AMVN (0.5 mM) for 2 h. Typical results of 4 performed experiments are shown. In all experiments, * designates statistically significant ($p<0.05$) differences from control.

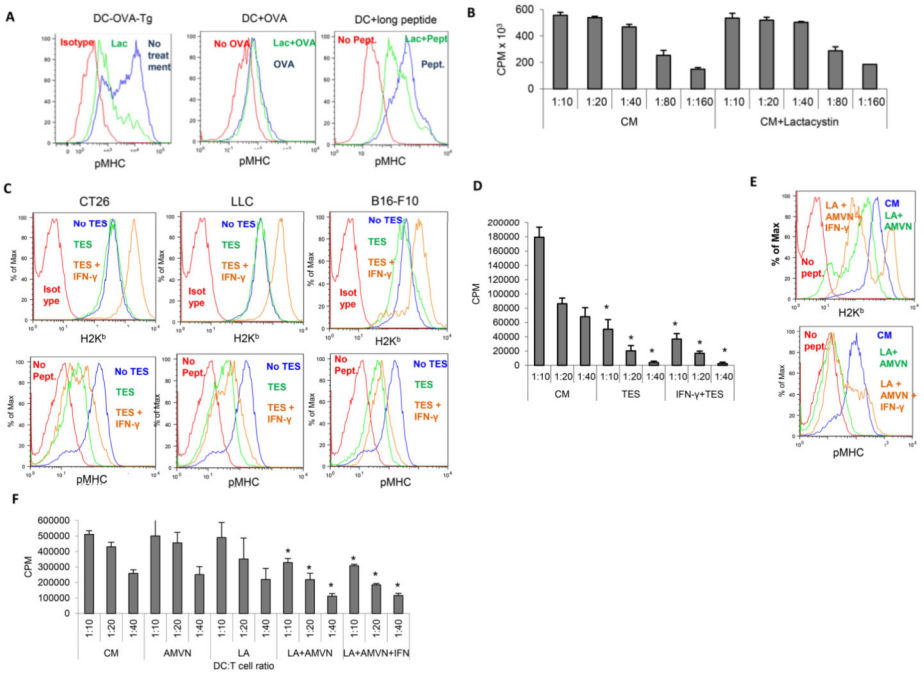

Figure 8. The mechanisms of oxidized lipids effect on cross-presentation by DCs

A. pMHC expression on DCs treated with 5μM of proteasome inhibitor lactacystin for 48 h. Wild-type DCs were directly loaded with 100 μg/ml OVA or 5μg/ml long OVA-derived peptide, during the last 24 h of culture, in the presence of lactacystin. Two experiments, with the same results were perfroemd. **B.** The effect of lactacystin on the ability of DCs, loaded with OVA (100μg/ml), to stimulate proliferation of OT-1 T cells. **C, D.** The effect of IFN-γ on cross-presentation of long OVA-derived peptide, by DCs treated with TES. DCs were cultured with IFN-γ (250 ng/ml) for 1 day, followed by TES treatment and loading with long OVA-derived peptide. **C.** Top panel – pMHC expression; bottom panel MHC class I ($H2K^b$) expression. CT26, LLC, and EL-4 designate type of TES used. **D.** The effect of IFN-γ on the ability of DCs to stimulate proliferation of OT-1 T cells after loading with OVA. **E, F. T**he effect of IFN-γ on cross-presentation of DCs, loaded with LA and treated with AMVN. **E.** Top panel – MHC class I ($H2K^b$) expression; bottom panel - pMHC expression. **F**. The effect of IFN-γ on the ability of DCs to stimulate proliferation of OT-1 T cells after loading with OVA.